

INSTABILITY INDUCED MOMENTUM TRANSFER AT THE MARTIAN IONOPAUSE

U.V. Amerstorfer^{1,2}, T. Penz^{1,3}, N.V. Erkaev⁴, H.K. Biernat^{1,2,3}, H. Lammer¹

¹Space Research Institute, Austrian Academy of Sciences, Schmiedlstrasse 6, A-8042 Graz, Austria
(ute.amerstorfer@stud.uni-graz.at)

²Institute for Geophysics, Astrophysics, and Meteorology, University of Graz, Universitätsplatz 5, A-8010 Graz, Austria

³Institute for Theoretical Physics, University of Graz, Universitätsplatz 5, A-8010 Graz, Austria

⁴Institute for Computational Modelling, Russian Academy of Sciences, Ru-660036 Krasnoyarsk 36, Russia

Abstract. Pioneer Venus measurements of the velocity distribution in the magnetosheath near the terminator plane indicate that a viscous interaction takes place between the solar wind plasma and the upper atmosphere leading to a transfer of momentum from the solar wind to the ionosphere. Several spacecraft measurements (e.g. Phobos 2) of the Martian plasma environment can be interpreted in a similar way. We suggest that the Kelvin-Helmholtz plasma instability, which arises in higher latitudes at the Martian ionopause, is involved in transferring momentum from the solar wind to the ionosphere. Since the instability growth rate and wavelength are largest near the terminator plane, we assume that momentum transfer is most efficient there. By estimating the size of the interaction region from the wavelength, we calculate the velocity of the ionospheric particles. Compared with the planetary escape velocity, we conclude that this process may play a main role in the erosion of the Martian atmosphere, which will be studied in detail by the ASPERA-3 instrument onboard ESA's Mars Express spacecraft.

1. Observational evidence of ionospheric bubbles on Venus

Brace *et al.* (1982) have identified a number of characteristic ionospheric structures in the Venusian magnetosheath, like wavelike plasma irregularities or plasma clouds that are signatures of the solar wind-ionosphere interaction. Fig. 1 shows the location of these structures.

The wavelike structures are common across the entire dayside and are also found on the night side. In contrast, the clouds occur far more often on the night side, but are also found on the dayside, particularly in the morning. Since they are separated by an intervening region of magnetosheath plasma in a direction perpendicular to their flow direction, it is obvious that the source of these clouds lies far upstream of the terminator. A detailed analysis of the plasma within the clouds revealed that it is ionosphere-like in temperature and density. The observations of plasma clouds

indicate that plasma instabilities may be a main source for ionospheric erosion on Venus.

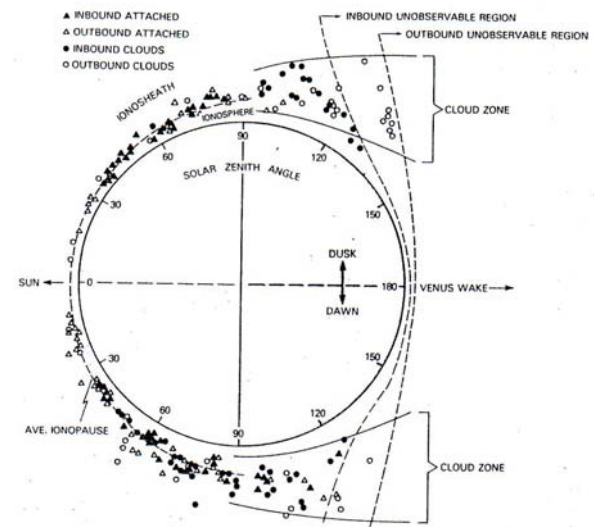


Figure 1. The distribution of attached plasma irregularities and clouds (after Brace *et al.*, 1982).

2. Ion outflow from Mars

Observations by the Soviet spacecraft Phobos 2 of the Martian plasma environment suggest that Mars is characterized by a strong loss of plasma from the topside ionosphere. This ion escape flow does not only contain light ions, but also molecular ion species, like O^+ , O_2^+ , or CO^+ (Lundin *et al.*, 1990). Mars Global Surveyor detected cold electrons above the Martian ionopause, which can also be interpreted as an indication for the presence of plasma clouds (Acuña *et al.*, 1998).

If plasma clouds, like those observed at Venus, are present also above the ionosphere of Mars, they are likely to be measured by the electron detectors of the

ASPERA-3 instrument on ESA's Mars Express spacecraft. The periapsis of Mars Express will be about 280 km, and as the orbit turns, the region above the ionopause will be probed for the whole range of solar zenith angles. The ASPERA-3 instrument is designed to measure electrons, atomic and molecular ions, and energetic neutral atoms with a complete coverage of the unit-sphere.

3. The Kelvin-Helmholtz instability

The fact that Mars has a very weak or no intrinsic magnetic field indicates that there is a direct interaction between the solar wind and the ionosphere. This implies a shear velocity between two different plasmas, which gives rise to the development of the Kelvin-Helmholtz (KH) instability.

Ideal MHD analysis of the KH-instability leads to the conclusion that the waves with the shortest wavelengths are the most unstable ones. However, by assuming a finite Larmor radius (FLR), we achieve a short-wavelength stabilisation of the boundary, whereas the consideration of gravity leads to a long-wavelength stabilisation (Fig. 2).

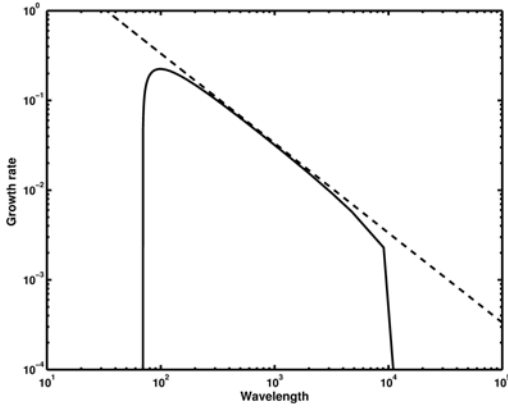


Figure 2. Growth rate of the KH-instability for gravity and FLR stabilisation (Penz *et al.*, 2004).

The growth rate is given by (Wolff *et al.*, 1980)

$$\gamma = \left(k^2 \frac{\rho_1 \rho_2 (v_2 - v_1)^2}{(\rho_1 + \rho_2)^2} + 2 |k|^3 \frac{(v_1 + v_2) \rho_1 \rho_2 (v_2 - v_1)}{(\rho_1 + \rho_2)^2} - k^4 \left(\frac{v_2 \rho_2 - v_1 \rho_1}{\rho_1 + \rho_2} \right)^2 - |k| \frac{g(\rho_2 - \rho_1)}{\rho_1 + \rho_2} \right)^{1/2}, \quad (1)$$

where k is the wave number, v is the flow velocity, g is the gravitational acceleration, ν is the viscous coefficient, and ρ is the density. Subscripts 1 and 2 denote the magnetosheath and the ionosphere, respectively. It is important to compare the instability growth time t with the time scale of the magnetic barrier formation time t_M , which can be estimated as the time needed for the transport of a frozen-in magnetic field line from the bow shock to the ionopause.

If $t < t_M$, then the instability may grow and plasma clouds can detach.

To model the solar wind flow around Mars we use a single-fluid, three-dimensional MHD model, which was successfully applied to the case of Venus (Biernat *et al.*, 2001). There are only a few spacecraft measurements to determine the plasma parameters at Mars. Since the KH-instability is assumed to arise near the terminator plane, we will consider two cases: near the polar terminator and near the equatorial terminator.

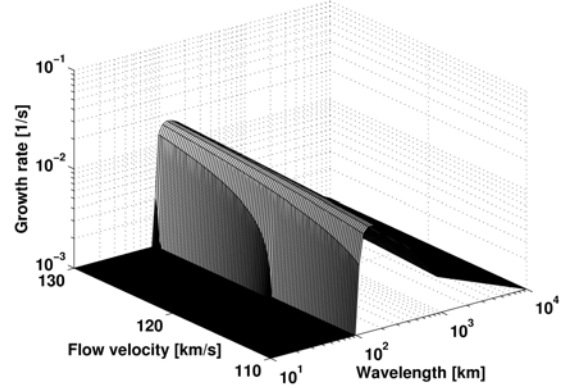


Figure 3. The growth rate for different flow velocities in the magnetosheath of Mars near the polar terminator (Penz *et al.*, 2004).

The ionospheric density n_2 in an ionopause altitude of about 400 km is about $8 \times 10^3 \text{ cm}^{-3}$, while the solar wind density n_1 is about 5 cm^{-3} . Near the polar terminator the magnetosheath velocity v_1 is found to be about 120 km/s. From these values, we can determine the viscous coefficients to be about $\nu_1 = 630 \text{ km}^2/\text{s}$ and $\nu_2 = 260 \text{ km}^2/\text{s}$ in the magnetosheath and in the ionosphere, respectively.

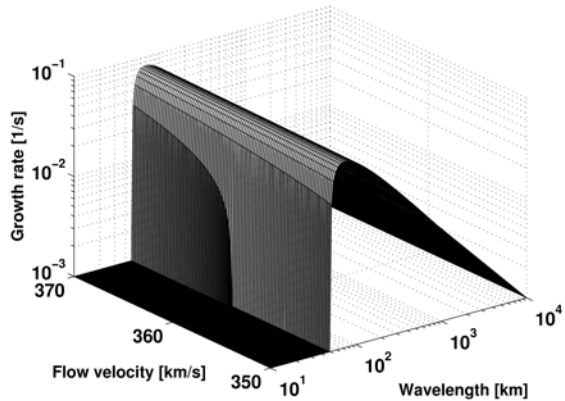


Figure 4. The growth rate for different flow velocities in the magnetosheath of Mars near the equatorial terminator (Penz *et al.*, 2004).

The maximum growth rate is about $\gamma = 10^{-2} \text{ s}^{-1}$ for wave-lengths of about 150 km, which is displayed in Fig. 3.

For the situation near the equatorial terminator we have a higher magnetosheath velocity v_1 of about 360 km/s. With the same ionospheric density the viscous

coefficients are about $v_1 = 5600 \text{ km}^2/\text{s}$ and $v_2 = 260 \text{ km}^2/\text{s}$ in the magnetosheath and in the ionosphere, respectively. The growth rate for this case is about $7 \times 10^{-2} \text{ s}^{-1}$ at wavelengths of about 60 km (Fig. 4).

For such small wavelengths, the finite boundary thickness must be taken into account. The assumption of a finite thickness of the boundary layer leads to the requirement that $kd/2 \approx 0.5$, where k is the wave number and d the boundary layer thickness (Ong and Roderick, 1972). If an ionopause thickness of about 20 km is assumed (Shinagawa and Bougher, 1999), wavelengths of about 120 km fulfil this requirement and the growth rate is still about $4 \times 10^{-2} \text{ s}^{-1}$ (Fig. 4).

4. Viscous processes triggered by the Kelvin-Helmholtz instability

An observed feature of the Venusian magnetosheath is a boundary layer, which is characterized by a depletion of energetic ions and downstream of the terminator by a decrease in the flow velocity and increase in the ion temperature, as in a viscous boundary layer. The idea of the presence of viscous-like processes in the solar wind-Venus interaction was widely examined (e.g., Pérez-de-Tejada, 1986; Pérez-de-Tejada, 1992). In this viscous interaction the solar wind transfers momentum to the ionosphere resulting in a decrease of the flow velocity and in an increase of temperature. A possible source of momentum transfer could be the nonlinear evolution of unstable density waves resulting from plasma instabilities within a region of a velocity shear (Pérez-de-Tejada, 1986).

In this study we will examine how the boundary layer and the velocities of the ionospheric ions depend on the quantities inferred from the KH-instability, such as the wavelength and amplitude. First of all, we consider only the region near the terminator plane, where the KH-instability is found to be the largest, and thus the momentum transfer should be most effective there. This restriction allows us to formulate the problem in a plane geometry, neglecting curvature effects (Fig. 5).

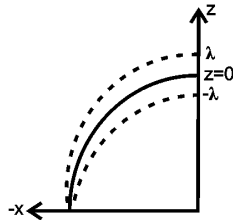


Figure 5. Geometry of momentum transfer near the terminator plane. The boundary layer width grows with increasing distance to the subsolar point.

Since mass and momentum flux conservation should be valid, we get

$$\int_0^{\lambda} \rho'_{sw} v'_{sw} dz = \int_{-\lambda}^{\lambda} \rho_{sw} v_{sw} dz, \quad (2)$$

$$\int_0^{\lambda} \rho'_{sw} v'^2_{sw} dz = \int_0^{\lambda} \rho_{sw} v^2_{sw} dz + \int_{-\lambda}^0 \rho_i v_i^2 dz, \quad (3)$$

where ρ'_{sw} and v'_{sw} are the solar wind density and velocity in the magnetosheath, respectively, ρ_{sw} and v_{sw} are the solar wind density and velocity near the ionopause due to the viscous interaction, and ρ_i and v_i are the density and velocity of the planetary ions in the upper ionosphere, respectively. Quantity λ denotes the specific wavelength of the KH-instability, at which plasma clouds can detach, and defines the region where the viscous interaction takes place, i.e. the boundary layer width, and dz is a path element in z -direction. Equation (2) represents the mass conservation and Equation (3) the momentum flux conservation. Assuming constant values and rewriting these two equations we get

$$\rho'_{sw} v'_{sw} \lambda = \rho_{sw} v_{sw} 2\lambda, \quad (4)$$

$$(\rho'_{sw} v'^2_{sw} - \rho_{sw} v^2_{sw}) \lambda = \rho_i v_i^2 \lambda, \quad (5)$$

where λ can be cancelled, but still plays an important role in determining the escape rate of the accelerated ions since λ gives the radius of the cross section through which the accelerated ions will escape. After rewriting Equation (5) an expression for the ionospheric velocity is obtained

$$v_i^2 = v'^2_{sw} \frac{\rho'_{sw}}{\rho_i} \left(1 - \frac{\rho_{sw} v^2_{sw}}{\rho'_{sw} v'^2_{sw}} \right). \quad (6)$$

What we can see from this equation is, that the velocity v_i of the ionospheric particles increases with increasing v'_{sw} .

As already mentioned earlier, the solar wind parameters (density ρ'_{sw} and the velocity v'_{sw} of the solar wind in the magnetosheath) are taken from the results of a three-dimensional, single-fluid MHD model. Near the polar terminator we get $v'_{sw} = 120 \text{ km/s}$, and near the equatorial terminator $v'_{sw} = 360 \text{ km/s}$. The solar wind densities are approximately equal to the free-stream values, thus $n'_{sw} = 5 \text{ cm}^{-3}$. The density and velocity of the solar wind due to the viscous interaction are assumed to be $v_{sw} = 50 \text{ km/s}$ and $n_{sw} = 1 \text{ cm}^{-3}$ (Pérez-de-Tejada, 1992). The density of the oxygen ions, which dominate in the upper ionosphere, is taken to be $n_i = 500 \text{ cm}^{-3}$. Assuming a wavelength of about 100 km for the KH-instability gives a cross section of about $4.76 \times 10^{16} \text{ cm}^2$.

At the polar region, we obtain a velocity for the ionospheric particles of about $v_i = 2.3 \text{ km/s}$, which is below the escape velocity, but near the equatorial terminator

the velocity of the ions can reach about 6 km/s. Consequently, an O^+ escape rate of about $7 \times 10^{24} \text{ s}^{-1}$ was obtained, where the cross section was divided by two to roughly account for the fact that near the polar terminator no escape occurs.

5. Concluding remarks

If we compare the escape rate obtained by the present study of the momentum transfer from the solar wind to the upper ionosphere of Mars with escape rates of other processes, like ion pick-up, atmospheric sputtering or dissociative recombination processes (Lammer *et al.*, 2003), one can see that this process is definitely not negligible. Of course, this study is only a rough estimation and should be seen as a first step towards a better understanding of this process. The Martian plasma environment will be studied in detail by the ASPERA-3 instrument onboard ESA's Mars Express spacecraft, which will hopefully help to reduce several uncertainties contained in this study.

Acknowledgements. This work is supported by the Austrian "Fonds zur Förderung der wissenschaftlichen Forschung" under project P17099-N08, by grants No 04-05-64088 and No 03-05-20014 from the Russian Foundation of Basic Research, by grants E02-8.0-22 and A03-2.13-469 from the Russian Ministry of Higher Education, and by projects No. I.2/04 and No. I.12/04 from "Österreichischer Austauschdienst". Also acknowledged is support by the Austrian Academy of Sciences, "Verwaltungsstelle für Auslandsbeziehungen" and by the Russian Academy of Sciences.

References

- Acuña, M.H., et al., 1998. Magnetic field and plasma observations at Mars: Initial results of the Mars Global Surveyor mission, *Science*, 279, 1676.
- Biernat, H.K., N.V. Erkaev, and C.J. Farrugia, 2001. MHD effects in the Venus magnetosheath including mass loading, *Adv. Space Res.*, 28, 833.
- Brace, L.H., R.F. Theis, and W.R. Hoegy, 1982. Plasma clouds above the ionopause of Venus and their implications, *Planet. Space Sci.*, 30, 29.
- Lammer, H., H.I.M. Lichtenegger, C. Kolb, I. Ribas, E.F. Guinan, R. Abart, and S.J. Bauer, 2003. Loss of water from Mars: Implications for the oxidation of the soil, *Icarus*, 10, 23456.
- Lundin, R., A. Zakharov, R. Pellinen, S.W. Barabash, H. Borg, E.M. Dubinin, B. Hultqvist, H. Koskinen, I. Liede, and N. Pissarenko, 1990. ASPERA/Phobos measurements of the ion outflow from the Martian ionosphere, *Geophys. Res. Lett.*, 17, 873.
- Ong, R.S.B., and N. Roderick, 1972. On the Kelvin-Helmholtz instability of the Earth's magnetopause, *Planet. Space Sci.*, 20, 1.
- Penz, T., N.V. Erkaev, H.K. Biernat, H. Lammer, U.V. Amerstorfer, H. Gunell, E. Kallio, S. Barabash, S. Orsini, A. Milillo, and W. Baumjohann, 2004. Ion loss on Mars caused by the Kelvin-Helmholtz instability, *Planet. Space Sci.*, accepted.
- Pérez-de-Tejada, H., 1986. Fluid dynamic constraints of the Venus ionospheric flow, *J. Geophys. Res.*, 91, 6765.
- Pérez-de-Tejada, H., 1992. Solar wind erosion of the Mars early atmosphere, *J. Geophys. Res.*, 97, 3159.
- Shinagawa, H., and S.W. Bougher, 1999. A two-dimensional MHD model of the solar wind interaction with Mars, *Earth Planets Space*, 51, 55.
- Wolff, R.S., B.E. Goldstein, and C.M. Yeates, 1980. The onset and development of the Kelvin-Helmholtz instability at the Venusian ionopause, *J. Geophys. Res.*, 85, 7697.